OPERATIONAL PROCESS SIMULATION AND OPTIMIZATION OF A CONTINUOUS-DISCHARGE SYSTEM IN A BACKFILLING SYSTEM

OPERACIJSKA PROCESNA SIMULACIJA IN OPTIMIZACIJA KONTINUIRNEGA SISTEMA PRAZNJENJA V SISTEMU ZA POLNJENJE SILOSOV

Weicheng Ren[1,2], Shaohuai Wang[3], Rugao Gao[3*], Dengpan Qiao[4]

[1]North China University of Science and Technology, School of Mining Engineering, no. 21, Bohai Road, Tangshan 063009, Hebei, China
[2]North China University of Science and Technology, Key Laboratory of Mining and Safety Technology of Hebei Province, no. 21, Bohai Road, Tangshan 063009, Hebei, China
[3]Central South University, College of Resources and Safety Engineering, no. 932, Lushan Road (South), Hunan Changsha, Hunan, China, 410083
[4]Kunming University of Science and Technology, Faculty of Land and Resources Engineering, no. 68, Wenchang Road, Kunming 650093, China

In existing tailings-discharge (TD) systems, the feeding, settlement and discharge are conducted alternately in multiple vertical silos. A model of continuous TD, which differs from the aforementioned model, is proposed to solve the problems of the high fluctuation in underflow concentration and the relatively low, unstable actual discharge concentration in vertical tailings silos. The continuous discharge of the tailings in the silo was simulated using computational fluid dynamics software. In the simulation, four slurry-underflow conditions were selected to record the corresponding compression-region height and the variation of the slurry concentration with that height based on preset monitoring curves. In addition, a relationship between the tailings volume fraction and silo height was obtained by fitting, and a predictive model was proposed for the change in the volume fraction of the underflow tailings with the compression-region height. A new working mode of the discharge system in the backfilling system was proposed, and fluent software was used to simulate the new discharge system. Industrial field tests verified the reliability of the results of the numerical simulations. It greatly improved the work efficiency of the vertical silos as it reduced the number of working vertical silos, omitted the process of completely discharging and charging the silos, and simplified the preparation of the slurry materials. With these advantages, the model guaranteed the filling efficiency and quality. Applying the proposed model of continuous TD for vertical silos effectively overcame the technical problems facing the existing TD systems in mines.

Keywords: tailings, discharge system, continuous discharge, backfilling system, simulation

V obstoječem sistemu praznjenja rudarskih odpadkov oz. jalovine (TD; angl: tailings-discharge) se polnjenje, hramba in praznjenje jalovine izvaja v več vertikalnih silosih. Avtorji so za razliko od obstoječega modela predlagali nov model kontinuirnega TD, ki rešuje probleme velike fluktuacije v koncentraciji pretoka in relativno majhne nestabilne koncentracije materiala v vertikalnih silosih za jalovino. Kontinuirno praznjenje jalovine iz silosa so simulirali z uporabo programske opreme, izdelane na osnovi računalniško podprte dinamike fluidov. Za simulacije so izbrali štiri različne pogoje toka gošče jalovine, da bi ugotovili odgovarjajoče višine področij pod tlakom in variiranje koncentracije gošče z višino na osnovi obstoječih krivulj opazovanja. Dodatno so z računalniškim prilagajanjem ugotovili zvezo med volumskim deležem jalovine in višino silosa in predlagali model za napoved spremembe volumskega deleža jalovine v področjih oz. na višini s podtlakom. Predlagali so nov način delovanja sistema za praznjenje silosov z uporabniku prijazno simulacijsko programsko opremo. Pilotni industrijski preizkusi so potrdili zanesljivost rezultatov numeričnih simulacij. Močno se je izboljšala delovna učinkovitost vertikalnih silosov in tudi zmanjšalo se je njihovo število, ne da bi pri tem prišlo do motenj v procesu kompletnega praznjenja ali polnjenja silosov. Poenostavljena je bila tudi predpriprava jalovinskih materialov. S temi prednostmi model zagotavlja učinkovito polnjenje in njegovo kakovost. Z uporabo predlaganega modela za kontinuirno TD vertikalnih silosov so učinkovito rešili tehnične probleme obstoječega sistema praznjenja rudarskih silosov z jalovino.

Ključne besede: jalovina, vertikalni silos, sistem praznjenja, kontinuirno praznjenje, sistem ponovnega polnjenja, simulacija

1 INTRODUCTION

With the implementation of a sustainable development strategy in China, green mining technology has become the primary focus of technical innovation in mining.[1–4] Because of its safety, high recovery ratio and low impact on the surrounding environment, the backfill mining method has caused more mines to build filling systems to implement backfill mining.[5–6] As an integral part of a filling system, vertical silos (VSs) can load, store and discharge tailings slurry (TS). The discharge of the tailings from VSs is important, and its underflow concentration and slurry flow regime affect the efficiency and costs of filling. However, various problems are faced by the existing methods for tailings discharge (TD); for example, multiple silos working simultaneously to discharge tailings alternately, discharge underflow requiring secondary slurry, and the underflow concentration appreciably fluctuating, making it difficult to control. Using fewer VSs and maximizing their
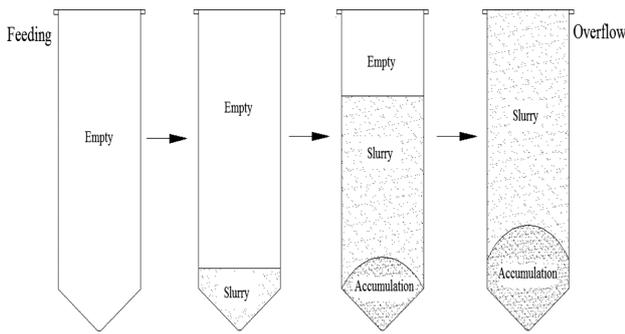
Figure 1: Process of filling silo with tailings slurry (TS)

efficiency cannot only save on infrastructure, water and electricity costs considerably, but also improve the uniformity and density of the fill under working conditions. Therefore, research on VSs must be conducted. Some progress has been made in research into the dynamic sedimentation of the tailings in thickeners.[7–14]

A tailings silo involves the process of loading tailings before discharging the slurry. As shown in **Figures 1** and **2**, this can be divided into two separate processes to reflect the actual situation, i.e., (i) filling the silo with TS and (ii) tailings accumulating in the silo. To date, most studies on VSs have been aimed at improving the discharging slurry concentration. The direction of such research involves optimizing the structure of the tailings silo and developing new nozzles. Deep cone thickeners are now explained by a relatively complete theoretical system, but not so related applications for VSs. In the existing TD systems, feeding, settlement and discharge are alternately conducted in multiple VSs. A continuous TD model, which differs from the existing models, is established, and **Figure 3** shows the two different continuous-discharge scenarios.

2 MATERIALS AND METHODS

2.1 Materials

The tailings used for the experiments were collected from the first filling station in the Dahongshan copper mine in Yuxi, located in Yunnan Province, China. The
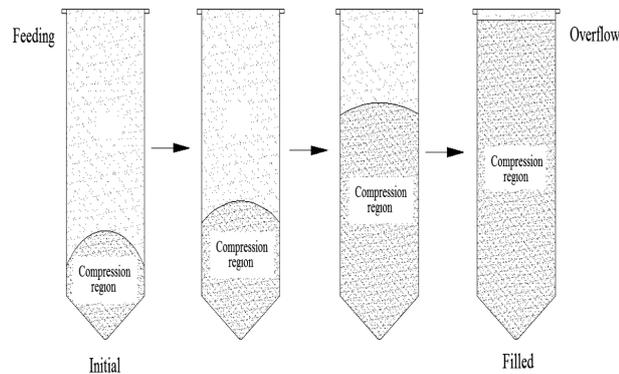

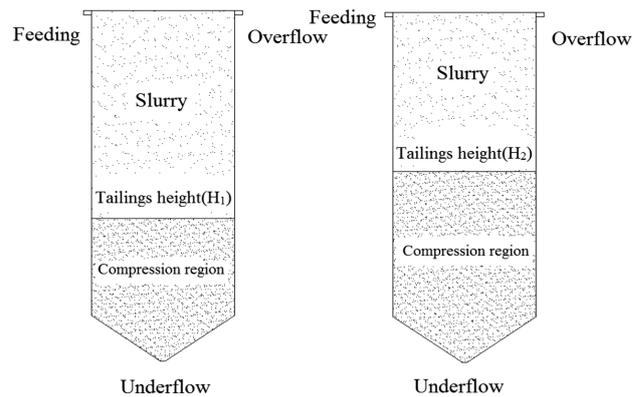**Figure 2:** Process of tailings accumulating in the silo

Figure 3: Model of continuous discharge

main physical properties were measured using specific methods and instruments, and the chemical composition was measured using X-ray fluorescence spectral analysis (the tests were performed at the Ministry of Education Key Laboratory of Orogenic Belts and Crustal Evolution at Peking University). The main physical properties and the chemical constituents are listed in **Tables 1** and **2**, respectively.

Table 1: Physical properties of the tailings

Porosity (%)	Average particle size (mm)	Permeability coefficient (cm/h)	Specific gravity (g/cm³)
43.04	0.1165	0.9	2.897

Table 2: Chemical constituents of the tailings

Component	Content (%)	Component	Content (%)
SiO_2	76.37	Na_2O	0.09
TiO_2	0.17	K_2O	0.04
Al_2O_3	0.68	Total oxide	86.177
Fe_2O_3	5.83	LOI	13
MgO	0.44	Ni	0.0988
MnO	0.007	Cu	0.0451
P_2O_5	0.16	Co	0.0082
CaO	2.39	Cr	0.5606

As listed in **Table 2**, the main chemical constituents of the tailings are SiO_2, Fe_2O_3, and CaO. The contents of SiO_2 and Fe_2O_3 are more than 82 %, which could improve the later strength of the backfill. The content of CaO is 2.39 %, indicating that the tailing has a small amount of activity. The content of recycled metal is relatively low, and poisonous or harmful elements are present in traces or absent in the minerals. An analysis shows that the tailings are made of inert materials and meet the selection conditions for mining filling materials.

2.2 Grading tests

The tailings were divided into seven graded groups, i.e., +100 mesh, –100 + 200 mesh, –200 + 325 mesh, –325 + 400 mesh, –400 + 500 mesh, –500 + 625 mesh,

and –625 mesh. The tailings of each particle size were weighed after screening. **Table 3** lists the measured proportion of tailings for each particle size. The –325 + 400 mesh, +500 – 400 mesh, and 500 – 625 mesh groups had relatively low proportions of tailings and therefore were incorporated into the –625 mesh group with a total proportion of 31 %.

Table 3: Grading of all the tailings from the Dahongshan copper mine

Mesh	Percent (%)
+100	24
−100+200	23
−200+325	22
−325+400	8
−400+500	5
−500+625	1
−625	17
Total	100

2.3 L-pipe tests

L-pipe tests were conducted in the Dahongshan copper mine of the Yuxi Mining Co., Ltd. The slurry volume concentration was varied as 0.5271, 0.5271, 0.5421, and 0.5703. **Figure 4** shows a photograph of one L-pipe test. The stowing gradient is 6.8, based on the actual situation in the mine.

2.4 Computational fluid dynamics (CFD) simulation

Geometrical model

A geometrical model was established based on the actual size of the tailings silo, which was 9.0 m in diameter and 23.0 m in height. The feeding mouth was located 1.5 m from the top surface center and was set to overflow the mouths on the top. The underflow mouth was located at the bottom of the cone. **Figure 5** shows the geometrical model of the silo.

The mixture model was established to obtain the standard k–ε epsilon solution.[15–16] The acceleration due to gravity was set to 9.8 m/s²; the primary phase was liquid with a density of 998 kg/m³, and the secondary phase was solid with a density of 2.897 kg/m³. The solid phase of the tailings was divided into four groups based

Figure 4: Photograph of the L-pipe test

on the screening results. During the screening experiments, the percentage of each particle group was determined based on the actual measurements of the tailings' particle size. Each grade was assigned an average particle size, and the volume fraction of each particle-size category was calculated as given in **Table 4**.

Table 4: Settings of the solid granular phase

Diameter, mm	0.165	0.1195	0.0605	0.0335
Percent, %	24	23	22	31
Volume fraction	0.0312	0.0299	0.0286	0.0403

2.4.1 Calculation equations

1) The continuity equation for the mixture is as follows:

$$\frac{\partial}{\partial t}(\rho_m) + \nabla \cdot (\rho_m \vec{v}_m) = \dot{m} \tag{1}$$

Where $\dot{m}$ is the mass transfer, kg; $\vec{v}_m$ is the average velocity, m/s; ρ_m is the mixture density.

2) The momentum equation for the mixture is as follows:

$$\frac{\partial}{\partial t}(\rho_m \vec{v}_m) + \nabla \cdot (\rho_m \vec{v}_m \vec{v}_m) = -\nabla p + \nabla \left[\mu_m (\nabla \vec{v}_m + \nabla \vec{v}_m^T) \right]$$
$$+ \rho_m \vec{g} + \vec{F} + \nabla \cdot \left(\sum_{k=1}^{n} \alpha_k \rho_k \vec{v}_{dr.k} \vec{v}_{dr.k} \right) \tag{2}$$

where n is the phase number; $\vec{F}$ is the body force, N/m³; μ_m is the mixture viscosity, Pa/s⁻¹; $\vec{v}_{dr.k}$ is the drift velocity of the second phase, m/s; α_k is the volume fraction of the k phase.

2.4.2 Boundary conditions

1) A doubly symmetric plane was used to reduce the computing time and save the computing resources. Cal-
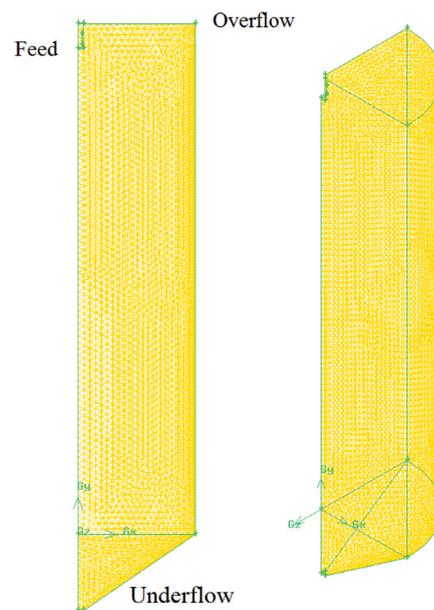
Figure 5: Geometrical model of the silo

culations were conducted on a grid covering only a quarter of the volume of the tailings silo. The wall was stationary and subject to the no-slip boundary condition.[17,18]

2) Free export was used at the overflow outlet face.

3) The TS had a volume concentration of 0.13 and a speed of 3.276 m/s at the feeding inlet face. The velocity (v_f) function is given below:

$$v_f = \frac{4Q_f}{3600\pi D_f^2} \qquad (3)$$

where Q_f is the slurry feeding ability (m³/h) and was equal to 300 m³/h, and D_f is the diameter of the inlet face and was equal to 0.179 m.

4) The underflow outlet face was set velocity outlet. The velocity (v_u) function is given below:

$$v_u = \frac{4Q_u}{3600\pi D_u^2} \qquad (4)$$

where Q_u is the slurry-underflow ability (m³/h) and was equal to (74, 72, 70, and 68) m³/h, and D_u is the diameter of the inlet face and was equal to 0.179 m. The corresponding slurry-underflow velocity was (0.291, 0.283, 0.275, and 0.267) m/s, respectively.

5) A gravity field was applied in the calculation domain, and standard atmospheric pressure (1 bar) was used as the reference atmospheric pressure.
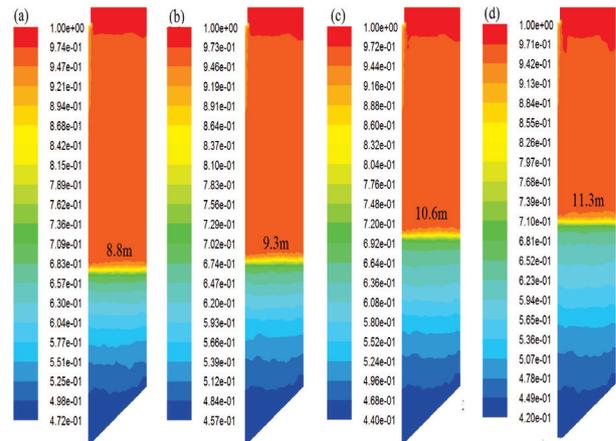
3 RESULTS AND DISCUSSION

3.1 CFD simulation results

The contours of tailings density and water volume drawn from the results of the numerical simulations are shown in **Figures 6** and **7**, respectively. **Figure 8** shows
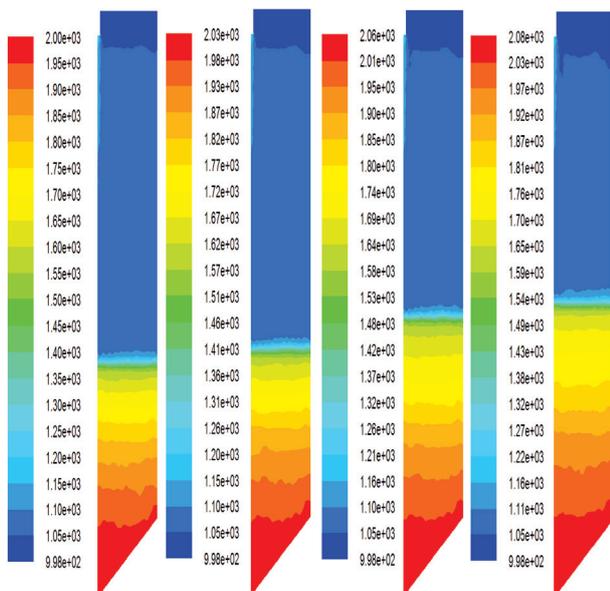
Figure 6: Density contours of tailings for different heights of the compression region (CR)

Figure 7: Contours of the volume fraction of water phase with interface levels of: a) 8.8 m, b) 9.3 m, c) 10.6 m, and d) 11.3 m

the distributions of the particle volume fraction for the diameters of (0.165, 0.1195, 0.0605 and 0.0335) mm.

Figures 6 and **7** show that a dynamic balance can be achieved for different heights of the compression region (CR), when feeding, underflow and overflow remain stable. The greater the height of the CR, the higher the volume fraction of the underflow.

Figure 8 shows the distributions of the volume fraction for the four tailings particle sizes.

3.2 Analysis of the simulation results

1) The following conclusions were obtained by comparing the distributions of the volume fraction for the four tailings particle sizes. As is well known, the coarser tailings particles settle faster than the finer backfilling particles. Therefore, the distributions demonstrated a hierarchical pattern because of the natural gradation that occurs in a VS. The volume fraction was concentrated at the bottom of the compression region (CR), whereas the 0.165 and 0.1195 mm tailings and the particle phases 0.0605 and 0.0335 mm in diameter were concentrated in the middle-to-upper part of the CR.

2) CFD software was used to simulate the underflow volume concentration as a dynamic balance. The obtained heights of the CR were (8.8, 9.3, 10.6, and 11.3) m for a feeding ability of 300 m³/h and underflow abilities of (74, 72, 70, and 68) m³/h, respectively. As listed in **Table 5**, the simulations achieved accurate underflow volume concentrations for the four CR heights via the monitoring curve (i.e., 0.5271, 0.5421, 0.5582, and 0.5703, respectively).

Table 5: Underflow concentrations for different heights of the CR

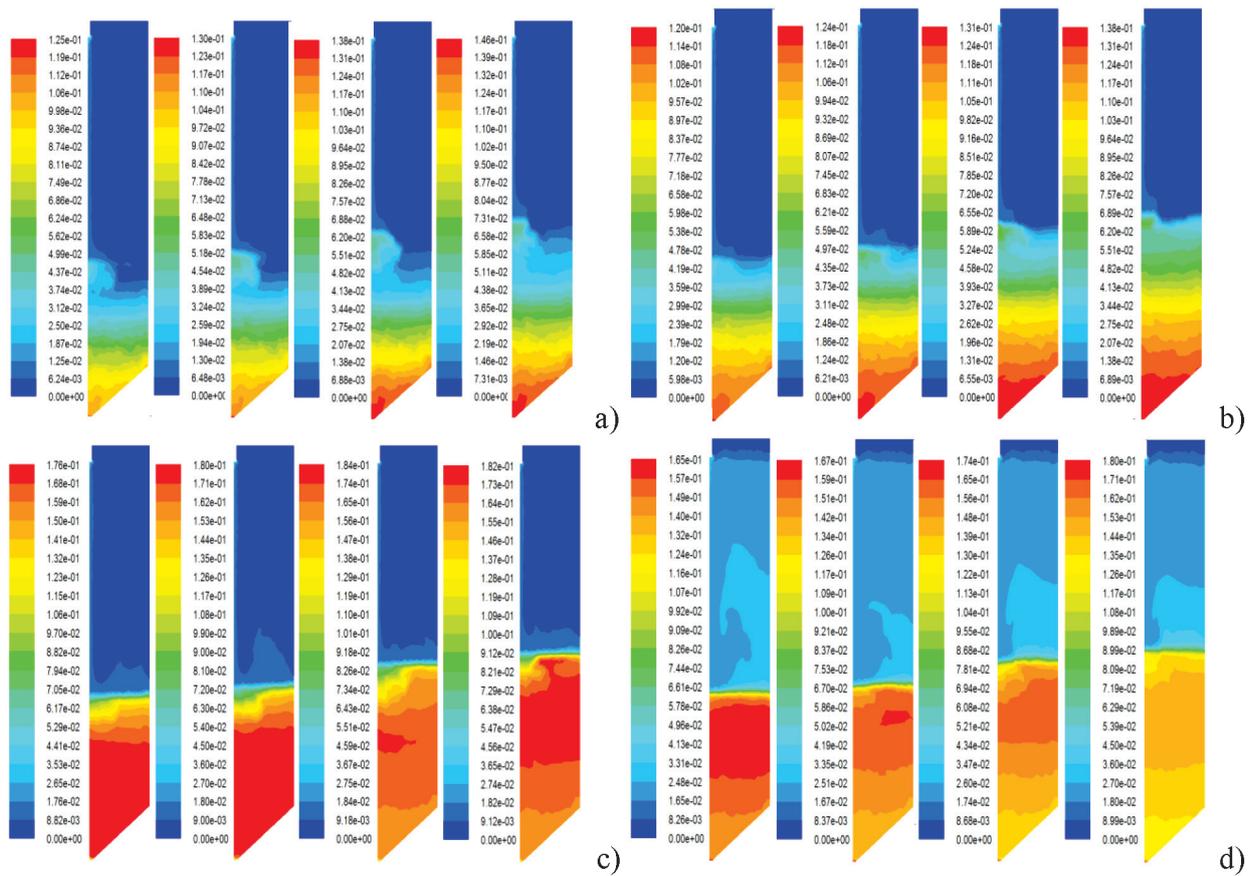| Q_f(m³/h)	Q_u(m³/h)	Compression area height(m)	Underflow volume concentration
300	74	8.8	0.5271
	72	9.3	0.5421
	70	10.6	0.5582
	68	11.3	0.5703

Figure 8: Contours of the volume fraction of the particle phase for diameters of: a) 0.165 mm, b) 0.1195 mm, c) 0.0605 mm, and d) 0.0335 mm

3) The relationship between the height of the CR and the underflow concentration was recorded using monitoring curves. **Figure 9** shows that an exponential relationship could be established between the underflow concentration as the abscissa and the height of the CR as the ordinate.

The following predictive model can be proposed by analyzing the way in which the volume fraction of an underflow backfilling material changes with the height of the CR:

$$x = a\overline{d}e^{(-\varphi/b)} + c\rho \qquad (5)$$

where x is the height of the CR (m), ϕ is the tailings volume fraction, $\overline{d}$ is the average tailings particle size (mm) and was equal to 0.1165 mm, ρ is the tailings density (g/cm³) and was equal to 2.897 g/cm³, and a, b, and c are the fitting parameters. The values of the volume fraction and height were then substituted into the predictive model, and **Table 6** illustrates the results of fitting Equation (1).

Table 6: Fitting equation relating the tailings volume fraction to the height of the CR for heights of (8.8, 9.3, 10.6, and 11.3) m

Height of the compression region (m)	Fitting equation	R^2
8.8	$x = -0.292\overline{d}e^{(\varphi/0.095)} + 3.22\rho$	0.977
9.3	$x = -0.63\overline{d}e^{(\varphi/0.11)} + 3.95\rho$	0.987
10.6	$x = -2.15\overline{d}e^{(\varphi/0.14)} + 4.99\rho$	0.992
11.3	$x = -3.09\overline{d}e^{(\varphi/0.15)} + 5.79\rho$	0.996
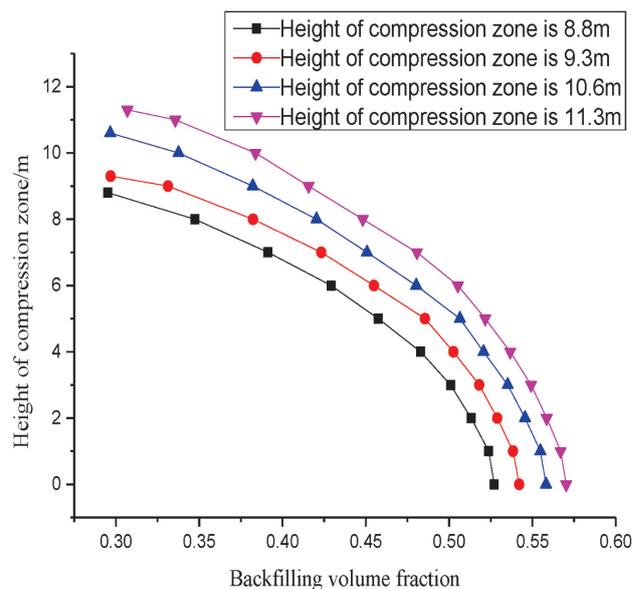
Figure 9: Variation of slurry concentration with height of CR

3.3 Analysis of L-pipe tests

L-pipe tests were conducted with TS volume concentrations of 0.5271, 0.5271, 0.5421 and 0.5703. The tests for volume concentrations of 0.5271 and 0.5271 could be completed smoothly, but the pipe was prone to blocking at concentrations of 0.5582 and 0.5703. The blockages were due to the excessive amounts of backfilling material in the slurry solution. The particles settled faster than the water flowed, so it was not the conditions of the pipeline transport. Hence, the industrial tests of TS discharge were conducted for TS volume concentrations of 0.5271 and 0.5421 only.

3.4 Industrial tests

Industrial tests were conducted in August 2016 using the 9-m tailings silo of the first filling station in the aforementioned Dahongshan copper mine. The feeding flow ability was controlled at 300 m³/h, and the volume concentration was maintained at approximately 13 %. The height of the CR was measured with a measuring tape. The gate at the bottom of the tailings silo was opened, and the TS was discharged for CR heights of

Figure 10: Photograph of an industrial test

Table 7: Industrial test of continuous underflow for a CR height of 8.8 m

Time	Feeding slurry weight (g)	Feeding slurry volume concentration	Underflow slurry weight (g)	Underflow slurry volume concentration	compression region height (m)
15:40	965	0.135	1342	0.493	8.8
15:50	959	0.129	1378	0.527	8.8
16:00	963	0.133	1392	0.540	8.8
16:10	955	0.125	1388	0.537	8.7
16:20	962	0.132	1381	0.530	8.7
16:30	966	0.136	1376	0.525	8.7
16:40	957	0.127	1368	0.518	8.7
16:50	960	0.130	1379	0.528	8.7
17:10	963	0.133	1382	0.531	8.6
17:20	966	0.136	1371	0.520	8.6
17:30	965	0.135	1366	0.516	8.6
17:40	953	0.123	1379	0.528	8.6
17:50	957	0.127	1374	0.523	8.6
18:00	959	0.129	1369	0.519	8.6
18:10	962	0.132	1377	0.526	8.6
18:20	964	0.134	1384	0.533	8.6
18:30	966	0.136	1374	0.523	8.6
18:40	964	0.134	1372	0.521	8.6
18:50	956	0.126	1369	0.519	8.6
Average	961.16	0.131	1374.789	0.524	

On August 10, 2016 in φ9 m-2# tailings silo

Table 8: Industrial test of continuous underflow for a CR height of 9.3 m

Time	Feeding slurry weight (g)	Feeding slurry volume concentration	Underflow slurry weight (g)	Underflow slurry volume concentration	Compression region height (m)
8:30	963	0.133	1358	0.508	9.3
8:40	966	0.136	1398	0.546	9.3
8:50	968	0.138	1401	0.549	9.2
9:00	953	0.123	1395	0.543	9.2
9:10	955	0.125	1393	0.541	9.2
9:20	971	0.141	1384	0.533	9.2
9:30	967	0.137	1381	0.530	9.2
9:40	962	0.132	1390	0.539	9.2
9:50	966	0.136	1397	0.545	9.2
10:00	958	0.128	1395	0.543	9.2
10:10	952	0.123	1391	0.539	9.2
10:20	956	0.126	1383	0.532	9.2
10:30	951	0.122	1388	0.537	9.2
10:40	958	0.128	1395	0.543	9.2
10:50	957	0.127	1398	0.546	9.2
11:00	963	0.133	1393	0.541	9.2
11:10	967	0.137	1387	0.536	9.2
11:20	969	0.139	1384	0.533	9.2
11:30	959	0.129	1391	0.539	9.2
11:40	952	0.123	1395	0.543	9.2
11:50	962	0.132	1392	0.540	9.2
12:00	968	0.138	1397	0.545	9.2
12:10	965	0.135	1390	0.539	9.2
12:20	963	0.133	1386	0.535	9.2
12:30	967	0.137	1384	0.533	9.2
Average	961.52	0.132	1389.84	0.538	

On August 12, 2016 in φ9 m-4# tailings silo

8.8 m and 9.3 m and underflow abilities of 74 m^3/h and 72 m^3/h, respectively. The accumulation of the tailings at the bottom of the silo was kept appropriately loose using high-pressure air and water at the start of TS discharge. **Figure 10** shows a photograph of one of the industrial tests. The underflow TS and the initial feeding concentration were simultaneously measured using a density pot. **Tables 7** and **8** provide detailed results.

Tables 7 and **8** indicate that the underflow volume concentration was stable at 0.524 and 0.538. The discharging ability of the underflow must be controlled to 74 m^3/h and 72 m^3/h when the height of the CR is 8.8 and 9.3 m, respectively. The results of the industrial tests are highly consistent with those of the CFD simulations. The volume concentration of the overflow at the top of the tailings silo was also measured during the industrial tests and was found to be less than 3 %.

4 CONCLUSIONS

The following conclusions can be drawn from the findings of the present study:

1) The volume fraction was concentrated at the bottom of the CR, whereas the 0.165 and 0.1195 mm tailings and the particle phases of 0.0605 and 0.0335 mm in diameter were concentrated in the middle-to-upper part of the CR.

2) Four underflow flow abilities (74, 72, 70, and 68) m^3/h were selected using CFD software when the feeding flow ability was 300 m^3/h. The results show that the CR height was 8.8, 9.3, 10.6, and 11.3) m when the underflow volume concentration was (0.5274, 0.5421, 0.5582 and 0.5703, respectively. A predictive model was proposed by analyzing the manner in which the underflow tailings volume fraction changed with the CR height, i.e., $x = ade^{(-\varphi/b)} + c\rho$.

3) The tests could be completed smoothly for TS volume concentrations of 0.5271 and 0.5421, but the pipe became blocked while testing at concentrations of 0.5582 and 0.5703.

4) Industrial tests demonstrated that the model worked and the underflow volume concentration met the requirements for mine production. Therefore, the model could be used to avoid wasting resources and equipment and to save water and electricity. The present research provides a theoretical basis and technical guidance for designing continuous TD and filling systems.

Acknowledgments

5 REFERENCES

[1] Q. L. Zhang, J. Q. Cui, J. J. Zheng, X. M. Wang, X. L. Wang, Wear mechanism and serious wear position of casing pipe in vertical backfill drill hole, T. Nonferr. Metal. Soc., 21 (**2011**) 11, 2503–2507, doi:10.1016/S1003-6326(11)61042-X

[2] K. P. Zhou, R. G. Gao, F. Gao, Particle flow characteristics and transportation optimization of superfine unclassified backfilling, Miner., 7 (**2017**) 6, doi:10.3390/min7010006

[3] X. M. Wang, J. W. Zhao, J. H. Xue, G. F. Yu, Features of pipe transportation of paste-like backfilling in deep mine, J. Cent. South. Univ., 18 (**2011**) 5, 1413–1417, doi:10.1007/s11771-011-08 55-7

[4] X. X. Zhang, D. P. Qiao, Simulation and experiment of pipeline transportation of high density filling slurry with coarse aggregates, T. Nonferr. Metal. Soc., 25 (**2015**) 1, 258–266, doi:1004-0609(2015)–01-0258-09

[5] H. David, A. Sebastian, R. Peter, Pipe lining abrasion testing for paste backfill operations, Miner. Eng., 22 (**2009**) 12, 1088–1090, doi:10.1016/j. mineng.2009.03.010

[6] R. Burger, Phenomenological foundation and mathematical theory of sedimentation consolidation processes, Chem. Eng. J., 80 (**2000**) 1, 177–188, doi:10.1016/S1383-5866(00)00089-7

[7] K. A. Landman, L. R. White, Solid/liquid separation of flocculated suspensions, Adv. Colloid Interfac., 51 (**1994**) 94, 175–246, doi:10.1016/00018686(94) 80036-7

[8] F. Betancourt, R. Burger, S. Diehl, Modeling and controlling clarifier thickeners fed by suspensions with time dependent properties, Miner. Eng., 62 (**2014**) 91–101, doi:10.1016/j.mineng.2013.12. 011

[9] F. Betancourt, R. Burger, S. Diehl, Advanced methods of flux identification for clarifier–thickener simulation models, Miner. Eng., 63 (**2014**) 4, 2–15, doi:10.1016/j.mineng.2013.09.012

[10] J. Kiventer, L. Golek, J. Yliniemi, V. Ferreira, J. Deja, M. Illikainen, Utilization of sulphidic tailings from gold mine as a raw material in geopolymerization, Int. J. Miner. Process., 149 (**2016**) 10, 104–110, doi:10.1016/j.minpro.2016.02.012

[11] A. Zeidan, S. Rohani, A. Bassi, Dynamic and steady-state sedimentation of polydisperse suspension and prediction of outlets particle size distribution, Chem. Eng. Sci., 59 (**2004**) 13, 2619–2632, doi:10.1016/j.ces.2004.01.064

[12] S. Diehl, Dynamic and steady-state behavior of continuous sedimentation, Siam J. Appl. Math., 57 (**1997**) 4, 991–1018, doi:10.1137/S00361399952 90101

[13] R. Font, P. Garcia, M. Perez, Analysis of the variation of the upper discontinuity in sedimentation batch test, Sep. Sci. Technol., 33 (**2008**) 10, 1487–1510, doi:10.1080/01496399808545062

[14] S. C. A. França, G. Massarani, E. C. Biscaia, Study on batch sedimentation simulation–establishment of constitutive equations, Powder Technol., 101 (**1999**) 2, 157–164, doi:10.1016/S0032-5910(98)00167-3

[15] Q. L. Zhang, Q. S. Chen, X. M. Wang, Cemented backfilling technology of paste-like based on aeolian sand and tailings, Miner., 6 (**2016**) 132, doi:10.3390/ min6040132

[16] D. A. White, N. Verdone, Numerical modelling of sedimentation processes, Chem. Eng. Sci., 55 (**2000**) 12, 2213–2222, doi:10.1016/S0009-2509(99)00496-0

[17] J. P. Chancelier, M. C. D. Lara, C. Joannis, F. Pacard, New insights in dynamic modeling of a secondary settler–I. Flux theory and steady-states analysis, Water Res., 31 (**1997**) 8, 1847–1856, doi:10.1016/S0043-1354(98)00002-5

[18] M. Rahimi, A. A. Abdollahzadeh, B. Rezai, The effect of particle size, pH and flocculant dosage on the gel point, effective solid stress and thickener performance of coal washing plant, Int. J. Coal Prep. Util., 35 (**2014**) 3, 125–142, doi:10.1080/19392699. 2014.996288